

# The function of zeolite on Pt autoreduction and dispersion in Pt/L and Pt/ $\beta$ catalysts

Jian Zheng<sup>a</sup>, Jialu Dong<sup>a</sup>, Qinhua Xu<sup>a</sup> and Cheng Hu<sup>b</sup>

<sup>a</sup> Department of Chemistry, Nanjing University, Nanjing 210093, PR China

<sup>b</sup> Laboratory of Solid State Microstructures, Nanjing University, Nanjing 210093, PR China

Received 8 May 1995; accepted 25 October 1995

TPR, CO-FTIR and  $^{129}\text{Xe}$  NMR spectroscopic techniques were used to measure the distribution of platinum species after the calcination of Pt/L and Pt/ $\beta$  zeolites. Autoreduction which occurred in Pt/ $\beta$  zeolite was avoided in the channel of L zeolite. Pt particles dispersed well and exhibited excellent reactivity for the aromatization of *n*-hexane in L zeolite.

**Keywords:** autoreduction; dispersion of Pt; L and  $\beta$  zeolites; *n*-hexane aromatization

## 1. Introduction

Since Pt supported on non-acidic KL or BaKL zeolite was found to be a highly active and selective catalyst for the aromatization of *n*-hexane, numerous significant studies have been conducted [1–7]. Several models describing the benzene formation [3,4] or hindered deactivation of metallic sites [5] in KL zeolite have been proposed to attribute to the unique channel structure of L zeolite. In contrast, Pt supported on the non-porous Mg(Al)O [6] has an aromatization selectivity similar to that of Pt/KL. Mielazarski et al. [7], based on their investigation, proposed that the uniqueness of Pt/KL for *n*-hexane aromatization was due to the ability of the L zeolite framework to stabilize extremely small Pt clusters in a completely non-acidic environment. However, the detailed catalytic mechanism is still not clear.

Recently, we studied directly the effect of autoreduction on Pt dispersion and catalytic activity over Pt/ $\beta$  zeolite [8]. We found that autoreduction resulted in the agglomeration of Pt atoms to larger Pt particles and subsequently caused the decreasing of the catalytic activity. Comparison of the acidic–basic properties and catalytic activities on Pt/ $\beta$  and Pt/L zeolites has also been carried out [9].

The purpose of this work is to study the function of zeolite in the reforming catalysts in more detail. Thus,  $^{129}\text{Xe}$  NMR spectroscopy combined with TPR and CO-FTIR was used to study the distribution of platinum species during the preparation and treatments of Pt/L and Pt/ $\beta$  zeolites. It is found that autoreduction does not occur during the calcination of  $\text{Pt}(\text{NH}_3)_2\text{Cl}_2/\text{L}$ , which results in the better Pt dispersion and excellent aromatization reactivity of Pt/L zeolite.

## 2. Experimental

### 2.1. Samples

L and  $\beta$  zeolites were obtained as described previously [9]. 0.6 wt% Pt/KL and Pt/K $\beta$  were prepared by dry impregnation of  $\text{cis-Pt}(\text{NH}_3)_2\text{Cl}_2$  in KL and K $\beta$  zeolites at 80°C. After Pt loading, the samples were dried at 110°C for 1 h, then kept in a desiccator.

### 2.2. Calcination

All samples were calcined in air in a packed bed reactor. The temperature was raised at 2°C/min from room temperature to a given temperature and then kept at this temperature for 1 h.

### 2.3. Temperature programmed studies

**TPR:** 0.05 g  $\text{Pt}(\text{NH}_3)_2\text{Cl}_2$  supported on KL or K $\beta$  zeolites were used. After calcination, each sample was cooled down to room temperature in  $\text{N}_2$ , then reduced in a flow of 5.5%  $\text{H}_2/\text{N}_2$  (30 ml/min). 5A molecular sieve was used to remove  $\text{H}_2\text{O}$  and  $\text{NH}_3$  formed during the TPR process. The temperature was increased to 500°C at 8°C/min.

**$\text{H}_2$ -TPD:** After the samples had been reduced, they were allowed to cool down to room temperature in  $\text{N}_2$ , then hydrogen was passed through the samples for 15 min. TPD experiments were carried out on these samples with a heating rate of 8°C/min in  $\text{N}_2$  gas.

### 2.4. CO-FTIR

$\text{Pt}(\text{NH}_3)_2\text{Cl}_2/\text{KL}$  zeolite was pressed into wafers (ca.

8 mg/cm<sup>2</sup>) and loaded into an in situ stainless-steel IR cell. When the calcination was over, the sample was cooled down in N<sub>2</sub> to room temperature, then CO gas was admitted at a pressure of  $4 \times 10^4$  Pa followed by purging with N<sub>2</sub>. CO-FTIR spectra were taken in a Nicolet 510P instrument at room temperature.

### 2.5. <sup>129</sup>Xe-NMR measurements

About 0.5 g pre-calcined sample was placed into an NMR tube. It was evacuated at 360°C for 2 h under  $10^{-3}$  Torr. Xenon gas (purity > 99.9995%) was introduced into the sample tube at room temperature. Then the NMR tube was sealed off with a flame. <sup>129</sup>Xe NMR spectra were obtained at room temperature with a Bruker 300MSL instrument operating at 83.010 MHz for <sup>129</sup>Xe. The chemical shift was referenced with respect to the chemical shift of xenon gas extrapolated to zero pressure.

### 2.6. Catalytic studies

Pt(NH<sub>3</sub>)<sub>2</sub>Cl<sub>2</sub>/KL and Pt(NH<sub>3</sub>)<sub>2</sub>Cl<sub>2</sub>/K $\beta$  catalysts were pelletized and screened between 20–40 mesh. In each run, 0.05 g catalyst on dry basis was placed in a pulse microreactor. All catalysts were calcined and then reduced with hydrogen at 500°C for 2 h. 0.4  $\mu$ l *n*-hexane was injected to the reactor at 500°C. The reaction products were analysed by on-line gas chromatography.

## 3. Results and discussion

### 3.1. TPR and CO-FTIR

The TPR spectra of Pt(NH<sub>3</sub>)<sub>2</sub>Cl<sub>2</sub>/KL after calcination at different temperatures ( $T_c$ ) are given in fig. 1. The  $T_r$  peak at 137°C, which was attributed to the reduction of Pt–ammine complexes [8], disappears after calcination at 300°C (spectrum c). This means that Pt(NH<sub>3</sub>)<sub>2</sub>Cl<sub>2</sub> complexes in KL zeolite decompose at this temperature which is the same as in K $\beta$  zeolite. The  $T_r$  peaks at 200–230°C and 420–430°C are the results of reduction of Pt<sup>2+</sup> ions located in the main channels and in some hidden sites of L zeolite, respectively.

We found previously [8] that after destruction of NH<sub>3</sub> ligands in the calcination step, a few platinum species other than Pt<sup>2+</sup> ions will appear in  $\beta$  zeolite. An additional broad TPR peak at about 270°C which was attributed to the reduction of PtO<sub>2</sub> appeared at 300°C calcination of Pt(NH<sub>3</sub>)<sub>2</sub>Cl<sub>2</sub>/K $\beta$  zeolite. A CO-FTIR band at 2088 cm<sup>-1</sup> was also found on the sample calcined at 310°C which indicated the appearance of Pt<sup>0</sup> atoms. Combination of the results of TPR and CO-FTIR made us believe that the removal of NH<sub>3</sub> groups in Pt(NH<sub>3</sub>)<sub>2</sub>Cl<sub>2</sub>/K $\beta$  zeolite may cause the autoreduction of Pt<sup>2+</sup> ions to form Pt<sup>0</sup> atoms, followed by oxidation of some Pt<sup>0</sup> to PtO<sub>2</sub> [8].

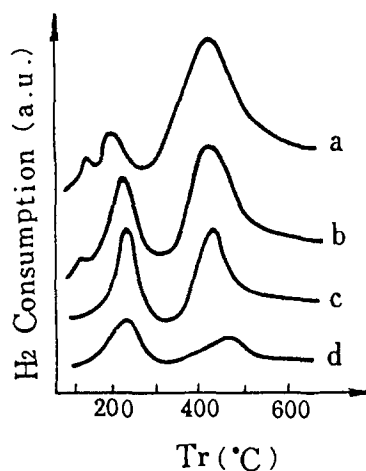


Fig. 1. TPR spectra of Pt(NH<sub>3</sub>)<sub>2</sub>Cl<sub>2</sub>/KL after calcination at (a) 110°C, (b) 250°C, (c) 300°C, (d) 400°C.

It is thus interesting to find that there is no peak at 270°C of Pt(NH<sub>3</sub>)<sub>2</sub>Cl<sub>2</sub>/KL zeolite on the spectrum c of fig. 1. Also, the CO-FTIR spectrum of Pt(NH<sub>3</sub>)<sub>2</sub>Cl<sub>2</sub>/KL after 300°C calcination is the same as that of KL zeolite. After subtraction of these two spectra, no CO-IR band in the range of 2000–2090 cm<sup>-1</sup> which indicates the appearance of Pt<sup>0</sup> atoms [8] is found (see fig. 2). These results reveal that no autoreduction occurs in Pt/KL zeolite under the same calcination treatment as for Pt/K $\beta$  zeolite.

### 3.2. <sup>129</sup>Xe NMR

<sup>129</sup>Xe NMR has been found to be a very sensitive probe of local environment inside the zeolite channel. In the case of <sup>129</sup>Xe adsorbed on zeolites, it is possible to obtain information on the dimensions of cavities and channels, the short distance crystallinity, the nature of structure defects, and finally, the effect of cations. While in the case of metal supported zeolites, the NMR spectrum of <sup>129</sup>Xe depends on the nature and concentration of the metal and the average number of atoms per particle [10].

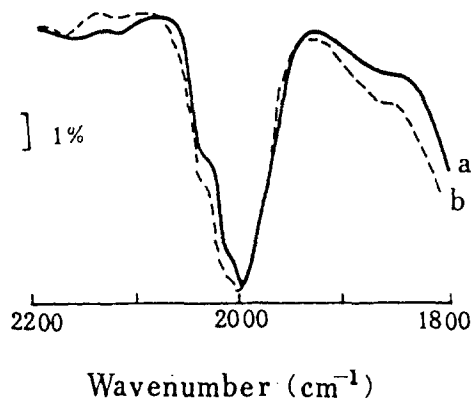


Fig. 2. CO-FTIR of (a) KL, (b) Pt(NH<sub>3</sub>)<sub>2</sub>Cl<sub>2</sub>/KL after calcination at 300°C.

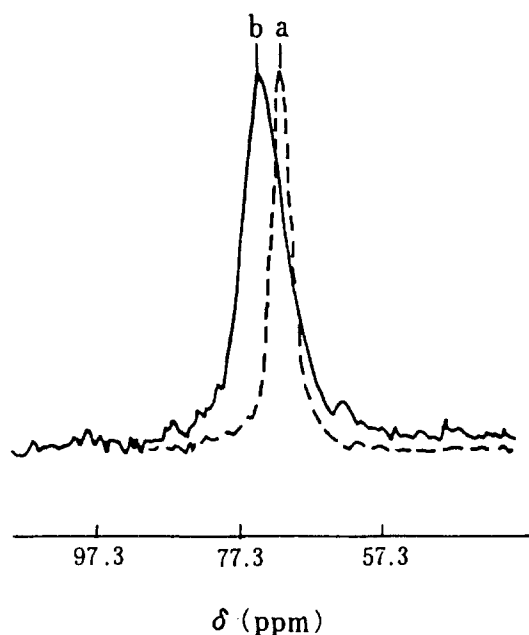


Fig. 3.  $^{129}\text{Xe}$  NMR spectra of  $\text{Pt}(\text{NH}_3)_2\text{Cl}_2/\text{K}\beta$  (a) with and (b) without calcination.

The  $^{129}\text{Xe}$  NMR spectra of  $\text{Pt}(\text{NH}_3)_2\text{Cl}_2/\text{K}\beta$  zeolite were obtained at  $2.9 \times 10^4$  Pa and room temperature. The samples were prepared with and without calcination at  $300^\circ\text{C}$  followed by  $360^\circ\text{C}$  evacuation (see fig. 3). The chemical shift of the sample with calcination (71.3 ppm) was smaller than that of the sample without calcination (73.6 ppm).

Due to the occurring of autoreduction, a few platinum species other than  $\text{Pt}^{2+}$ , such as  $\text{Pt}^0$  and Pt oxide, appeared in  $\text{Pt}(\text{NH}_3)_2\text{Cl}_2/\text{K}\beta$  zeolite during calcination. These different species might cause different chemical

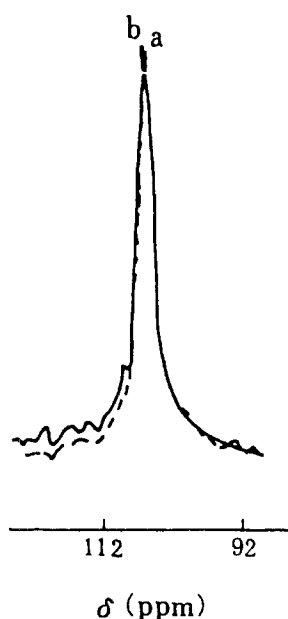


Fig. 4.  $^{129}\text{Xe}$  NMR spectra of  $\text{Pt}(\text{NH}_3)_2\text{Cl}_2/\text{KL}$  (a) with and (b) without calcination.

Table 1  
Pt dispersion (H/Pt ratio) of Pt/L zeolite by  $\text{H}_2$ -TPD

$T_c(^{\circ}\text{C})$	110	250	300	350	400
H/Pt	0.38	0.68	0.97	0.93	0.41

shifts. It was found [11] that  $\text{Pt}^{2+}$  polarized xenon atoms more strongly than the Pt oxide ( $\text{PtO}$ ) clusters did, therefore, the chemical shift caused by  $\text{Pt}^{2+}$  ions was smaller than that by Pt oxide. In our studies, the relative concentration of the various platinum species is strongly dependent on the preparation technique, which results in the change of chemical shift of  $^{129}\text{Xe}$  NMR.

Note that the chemical shift does not change after the same above treatments on Pt/KL zeolite (see fig. 4), which further indicates that no autoreduction occurs in Pt/L zeolite.

### 3.3. Pt dispersion and catalysis

Table 1 shows the results of  $\text{H}_2$ -TPD of  $\text{Pt}(\text{NH}_3)_2\text{Cl}_2/\text{KL}$  calcined at different temperatures. Since a larger H/Pt ratio means a smaller size of Pt particles, it is clear that the best dispersion of Pt particles is found on the sample calcined at  $300^\circ\text{C}$ .

Fig. 5 gives the benzene yield of *n*-hexane aromatization over Pt/KL and Pt/ $\text{K}\beta$  at different calcination temperatures. It is found that  $300^\circ\text{C}$  calcination does not show the maximum catalytic reactivity on Pt/ $\text{K}\beta$  zeolite where autoreduction occurs, while it does in Pt/KL zeolite. It is believed that *n*-hexane aromatization reactivity increases with decreasing Pt particle size [8]. Pt particles in KL zeolite after  $300^\circ\text{C}$  calcination are the smallest and result in the best catalytic reactivity. On the other hand, Pt/ $\text{K}\beta$  zeolite calcined at  $300^\circ\text{C}$  does not show maximum Pt dispersion and benzene yield. It is consistent with our previous results that Pt particles are better dispersed and exhibit much superior aromatization reactivity in Pt/KL than in Pt/ $\text{K}\beta$  zeolite [9].

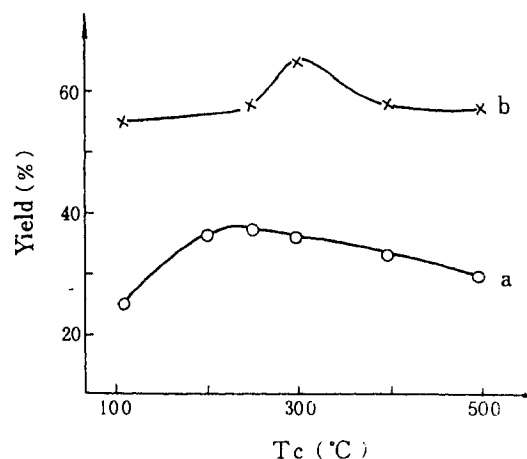


Fig. 5. Benzene yield of *n*-hexane aromatization over (a) Pt/ $\beta$  and (b) Pt/L zeolites (pulse flow microreaction, reaction temperature  $500^\circ\text{C}$ ).

#### 4. Conclusion

No autoreduction is found to occur on the  $\text{Pt}(\text{NH}_3)_2\text{Cl}_2/\text{KL}$  sample at 300°C calcination. Considering the structure of L and  $\beta$  zeolites, we believe that the unique unidimensional channel structure of L zeolite inhibits occurring of autoreduction and the agglomeration of Pt particles, and results in the best dispersion of Pt and the excellent catalytic behavior.

#### References

- [1] J.R. Bernard, *Proc. 5th Int. Conf. on Zeolites* (Heyden, London, 1980) p. 686.
- [2] T.R. Hughes, W.C. Buss, P.W. Tamm and R.L. Jacobson, *Stud. Surf. Sci. Catal.* 28 (1986) 725.
- [3] S.J. Tauster and J.J. Steger, *Mater. Res. Soc. Symp. Proc.* 111 (1988) 419.
- [4] E.G. Derouane and D.J. Vanderveken, *Appl. Catal.* 45 (1988) 419.
- [5] E. Iglesia and J.E. Baumgartner, *Proc. 10th Int. Congr. on Catalysis* (Elsevier, Budapest, 1993) p. 993.
- [6] R.J. Davis and E.G. Derouane, *Nature* 349 (1991) 313.
- [7] E. Mielazarski, S.B. Hong, R.J. Davis and M.E. Davis, *J. Catal.* 134 (1992) 359.
- [8] J. Zheng, J.L. Dong and Q.H. Xu, *Stud. Surf. Sci. Catal.* 82 (1994) 1624.
- [9] J. Zheng, J.L. Dong and Q.H. Xu, *Appl. Catal.*, to be published.
- [10] L.C. de Menorval, J.P. Fraissard and T. Ito, *J. Chem. Soc. Faraday Trans. I* 78 (1982) 403.
- [11] O.B. Yang, S.I. Woo and R. Ryoo, *J. Catal.* 123 (1990) 375.
- [12] W.M.H. Sachtler, *Catal. Today* 15 (1993) 419.